Desalination and Water Treatment
www.deswater.com
doi:10.5004/dwt.2017.20306

68 (2017) 80–90
March

Solar desalination of water using evaporation condensation and heat recovery method

Azlan Zahid[a], Abdul Ghafoor[a,*], Anjum Munir[b], Manzoor Ahmad[a], Abdul Nasir[c], Syed Amjad Ahmad[d]

[a]*Department of Farm Machinery and Power, Faculty of Agricultural Engineering and Technology, University of Agriculture, Faisalabad-Pakistan, Tel. +92 41 9200161-67 Ext. 3002, email: ch_azlan@hotmail.com (A. Zahid), ag_1272@yahoo.com (A. Ghafoor), manzoor.ahmad@uaf.edu.pk (M. Ahmad)*
[b]*Department of Energy Systems Engineering, Faculty of Agricultural Engineering and Technology, University of Agriculture, Faisalabad-Pakistan, Tel. +92 41 9200161-67 Ext. 3016, email: anjum.munir@uaf.edu.pk (A. Munir)*
[c]*Department of Structures and Environmental Engineering, Faculty of Agricultural Engineering and Technology, University of Agriculture, Faisalabad-Pakistan, Tel. +92 41 9200161-67 Ext. 3006, email: anawan@uaf.edu.pk (A. Nasir)*
[d]*NFC Institute of Fertilizer Research, Faisalabad-Pakistan, Tel. +92 300 6689867, email: samjadahmad67@yahoo.com (S.A. Ahmad)*

Received 21 March 2016; Accepted 31 October 2016

ABSTRACT

Desalination is a long term and reliable solution for increasing the fresh water supply but this process is consuming huge amount of primary energy. Fossil fuel reserves are diminishing and increasing fossil fuels combustion has also resulted severe climatic and environmental issues. In the meanwhile, the enormous amount of solar energy 5–5.5 kWh/m^2 in most parts of the Pakistan offers an excellent opportunity to use it effectively for desalination processes. This study has been carried out for the development and evaluation of solar desalination system using evaporation condensation and heat recovery method. The effect of key parameters on fresh water production have been studied and it was found that the fresh water productivity and system efficiency is a function of solar radiation, mass flow rates (MFR), tilt angle of flat plate collector (FPC) and inlet hot water temperature. The result shows that the daily specific fresh water productivity was found to be 4.5 l/m^2 with an overall system efficiency of 52%. The result also shows that the heat recovery of vapors in condensation chamber (CC) increases the system efficiency by 6% and the gain output ratio (GOR) of the system was found in the range of 1.7–2.2. The water quality tests show that the quality parameters are in line with WHO water quality standards and the concentration of arsenic, *E. coli* and facial coliform remained undetectable in the distillate. The cost per liter of water from the system was found to be $0.021 which is lower than the cost of the available bottled fresh water in the country.

Keywords: Solar collector; Desalination; Evaporation chamber; Condensation chamber; Distillate

1. Introduction

Water is the most important constituent of the atmosphere and it is essential for life on earth. Water covers major part of earth which is about three fourth of the whole planet. Conversely, about 97% water is salty in the oceans and only 3% is available in the form of fresh water. This 3% fresh water exists in glaciers, rivers, lakes and ground water that is used to fulfill the needs of human beings, animals etc. The water demand has increased both for domestic and industrial sector due to increasing population and better living standard around the world. About 1.1–1.5 billion people in the world lack access to good quality drinking water. A serious situa-

*Corresponding author.

tion prevails in Africa and Asia, where about 50% of the population do not have access to potable water [1]. According to World Health Organization (WHO), the harmful diseases produced from unsafe water supply, poor sanitation and hygiene causes about 1.8 million deaths annually in the world [2]. Similar conditions prevail in the coastal areas of Pakistan, where sea water is abundantly available but it is not potable. It is assessed that about one-fourth part to one-third of total population in Pakistan lack access to potable water supply. In the meanwhile, the desalination of sea water is a long term and reliable solution to increase fresh water supply, but this is an energy intensive process consuming huge amount of primary energy supply. For example, in order to produce 1000 m^3 desalinated fresh water on daily basis involves 10,000 tons of oil per year [3]. The previous studies show that desalination process can be classified as thermal and non-thermal based on the type of energy being consumed during this process [4,5]. The thermal desalination is carried out using heat energy from fossil fuels while the non-thermal is classified as reverse osmosis, vapour compression etc. requiring electrical energy in the range of 3–10 kWh/m^3 of distilled water [6]. According to an estimate, more than 14,000 desalination plants are in operation worldwide with gross capacity of billion liters of water per day. These desalination plants running with fossil fuels are becoming expensive and are also harmful to the environment due to harmful emissions. Furthermore, the limited reserves of fossil fuels and its environmental consequences has resulted desalination process as unsuitable and uneconomical for fresh water production [7]. In the meantime, the sustainable and environmental friendly renewable energy resources like solar, wind, hydel, biomass, geo-thermal etc. can be used as an attractive alternate for desalination process [8]. Out of these renewable energy sources, solar energy is also an economical fuel for desalination purpose because majority of countries have abundantly available solar radiation. It is also worth mentioning here that Pakistan is facing severe energy crisis from the last decade which has led the country to explore alternate sources of energy. Pakistan, being within the solar-drenched belt is lucky to have longer sunshine hours, enormous solar radiation and located ideally to take maximum benefit of solar energy both for thermal and PV electricity. In Pakistan, mean global irradiation ranges between 200–250W/m^2/d with annual sunshine hours of 1500–3000. The Baluchistan province receives maximum solar energy as compared with other provinces of the country and fresh water supply is the major issue in this area. It has an average insolation of 1.9–2.3 MWh/m^2/year making it an ideal location to use it for solar thermal applications [9].

The fresh water demand can be fulfilled if abundantly available saline sea water is converted to potable water using solar thermal energy for desalination process [10]. Solar energy is also an attractive opportunity to run desalination plants particularly in remote areas having lack of grid electricity and primary energy supply [11]. Solar assisted desalination has been proved theoretically feasible; however, integration of fossil fuel, solar and condensation heat recovery method could be more feasible and cost effective solution [12]. Among desalination options, the reverse osmosis (RO) is rapidly exceeding process in terms of market shares but it involves higher initial cost and energy requirement is also higher. Membranes aided RO can hold about 98–99% of the salts dissolved in the feed water within pressure range of 10–15 bars for brackish water and between 55–65 bars for seawater [13]. Many researchers around the world put their efforts to design and investigate thermal desalination systems. Integrated solar thermal desalination can be accomplished by two approaches either by passive (direct) or active (indirect) heating. The first approach uses an airtight basin type chamber containing feed water and is covered with a transparent glass rooftop. The top cover is slanted downward and directed towards the collection channels placed for distilled water. The greenhouse effect is used to vaporize saline water enclosed in the evaporation chamber [14]. The basin absorbs the solar energy that causes the water to vaporize and it is then condensed on the inner of the top cover and slips down into the distillate collection channel. Though simple, but the system has low collection efficiency typically in the range of 10–15% [15]. The direct methods require large areas and have relatively low water productivity as compared to indirect methods [16]. Solar water distiller is used for water distillation to produce high quality water. The losses are almost negligible contrasting RO process which wastes around 30% of inlet water [17].

A novel system integrated with solar collector having an area of 2.01 m^2 using falling film evaporation technology was developed [18]. The latent heat and sensible heat is successfully recycled to pre-heat the feedstock. Thermal performance of desalination system is significantly improved and the test showed that about 2–3-times higher yield was gained as compared with simple solar still system under the same climatic conditions. The performance of solar still in a new perspective for near zero liquid discharge (ZLD) desalination process was carried out to investigate the influencing meteorological parameters under hyper arid environment using different feed water sources. The system productivity, efficiency and operational recovery ratio reached 0.56 l/m^2/h, 52.38% and 36.77 respectively; for all sources while final recovery ratios were found to be 68, 93, and 95.6% for sea water, ground water, and drainage water respectively and R^2 was found to be in the range 88–96% using statistical modeling approach [19]. An integrated system covering a flash desalination technique coupled with nano-fluid based solar collector was investigated and it was found that the fresh water production of 7.7 l/m^2/d can be achieved with the cost of water as low as 11.68 US$/$m^3$ [20]. The water quality analysis (feed, product and brine) for the adsorption desalination (AD) plant was performed. The water quality test satisfied the EPA standards and the process is found to be effective in removing all type of salts, reducing TDS levels from 40,000 ppm in feed water to less than 10 ppm [21].

The second approach comprises more than one component, one for solar energy collection, second for energy storage and utilization during vaporization process and another for condensation by recovering the latent heat of vapors. Among the developed solar thermal desalination processes, evaporation and condensation by heat recovery method may offer a good option in terms of energy management and fresh water production for domestic purpose. Some researchers worked in order to increase the utilization of latent heat of condensation to increase efficiency and water productivity. A small integrated solar desalination system with multi-stage evaporation/heat recovery system

was developed which includes a heat exchangers (HEX) of copper tubes to recover latent heat of vaporization. The fresh water yield from the system reached 1.25 kg/h/m^2 with an overall system efficiency of 0.9 [22].

A new spray evaporation technique to improve water production by increasing the evaporation and condensation using 1 m^2 solar collector area was investigated and the result shows that, the maximum daily fresh water productivity reached 9 l/m^2 with daily system efficiency of 87% and has higher water productivity as compared to solar humidification–dehumidification (HDH) desalination system. The level of the total dissolved solids (TDS) in the fresh water was 40 ppm and the cost of distilled water was around $0.029 per liter [23]. Many studies have been conducted in the past to optimize the MFR. A study was conducted to evaluate and optimize the mass and heat transfer coefficients based on air HDH process for desalination of saline water. The results showed that the mean maximum inlet temperature of the evaporator was 71°C and the humid air mass flow rate was 0.05 kg/s. The authors reported that the daily maximum water productivity of the system reached up to 7.8 kg [24]. A hybrid desalination unit comprising of a one stage flashing evaporation unit and HDH unit was designed. The authors concluded that the maximum water productivity of the system was found to be 11.14 kg/m^2/d when the flow rate of water and air was set at 4.5 kg/s and 0.12–0.32 kg/s respectively [25]. The impact of air and water flow rates on distillate production of a designed solar HDH system was investigated and the authors found that the optimum flow rates of water and air was 0.005–0.045 kg/s and 0.0049–0.0294 kg/s respectively and maximum water productivity of the system reached up to 10.25 kg/d [26]. The effect of MFR on distillate productivity of the system was investigated and the results showed that at flow rates 0.012–0.023 kg/s (water) and 0.004–0.0043 kg/s (air), the system maximum productivity of 1.45 kg/h can be achieved [27]. The HDH cycle using design of experiment (DoE) method to achieve optimum operating conditions of the system was studied. The authors presented a thermodynamic analysis and energy balance equations for the humidifier and condenser. The optimum water and air flow rate was found to be 0.4–1.4 kg/s and 0.4–1.2 kg/s respectively. The simulated results showed that the maximum productivity reached 27 kg/h [28]. The cost of distilled water was found to be $0.107/L [29]. The effect of blackened surface and thermocol insulation on the performance of solar water distiller was studied and the authors concluded that the quantity of condensate was increased by 6.05% due to the blackened surface and thermocol insulation [30]. The above studies show that water spray is used during HDH process and carrier gas (air) is used to evaporate the feeding saline water in order to produce fresh water by condensation method. A 1 kg of dry air is capable to carry 0.5 kg of water vapors and 2805 kJ energy by increasing water temperature from 30 to 80°C [31]. It is therefore concluded that an efficient method for evaporation and condensation of water lies in low temperature range i.e. 70°C which can easily be achieved using low cost solar collector to perform thermal desalination. This study has been carried out for the development of a simple, low cost and easy to operate novel single stage integrated solar desalination system based on evaporation condensation and heat recovery method for domestic purpose in remote areas of the country where fresh water is not available or very costly. The whole system has been designed and developed using indigenous resources in order to decrease the initial cost and to increase the rate of evaporation at low temperature with copper tube HEX to improve its productivity and efficiency by the induction of heat recovery condensation chamber. The indigenization of solar thermal desalination technology will encourage the poor community to adopt this technology in order to get rid of primary energy sources and their contribution toward cleaner environment. The impact of influencing parameters like solar irradiance, tilt angle of FPC, MFR on heat transfer rate, performance and efficiency of the system under local climatic conditions was also the focus of this study. The water quality and economic analysis has also been carried out to determine the feasibility of the system.

2. Materials and methods

The solar desalination system consists of three major units namely evaporation chamber (EC), condensation chamber (CC) and flat plate collector (FPC). The schematic diagram of solar water distillation system is shown in Fig. 1.

A FPC having an area of 1 m^2 is the integral part of the desalination system. The FPC consists of copper tubes having an internal diameter and wall thickness of 4 and 0.4 mm respectively, an aluminum absorber plate having length and width of 1120 and 920 mm respectively and thickness of 0.5 mm. The black matt paint was sprayed over aluminum sheet as an absorber material. A 3 mm thick window glass was used as a cover material having a transmittance of 0.85. A 50 mm thick rock wool was used to insulate the system in order to reduce thermal losses. A GI–18 iron sheet (TC as 73 W/m/K) having thickness of 0.125 cm and specific weight as 10.52 kg/m^2 was used for the development of EC and CC units. The dimensions of EC and CC were selected as 76 cm × 76 cm × 22 cm and 76 cm × 76 cm × 18 cm respectively. The top cover of both the units/chambers was made pyramidal in shape each having total height of 18 cm. The copper tubes of 5 mm and 25 mm diameter (TC as 385 W/m/K) with a total length of 6250 mm and 3300 mm was used during the development of the HEX for EC and CC respectively. The inlet pipe of the system was connected with saline groundwater source. A thermocoal with 25 mm thickness (thermal conductivity as 0.007 W/m/K) was used to insulate the chambers to avoid thermal losses. A PVC pipe having 100 mm diameter was used in the desalination system for efficient transfer of water vapors from EC to CC. The FPC was oriented in the east-west direction to collect maximum solar radiation during the year. The FPC uses solar radiation to convert it into thermal energy using water as heating medium. The heat transfer fluid (water) is pumped in the copper pipes through FPC to the EC that act as a heat source for desalination system and a control valve is used to regulate the MFR. The circulation of hot water between FPC and EC is achieved using 12V DC pump operated with PV panel. Feed saline water coming from groundwater source to the EC is converted to vapors by exchanging heat with hot water passing through copper tubes. The vapors then

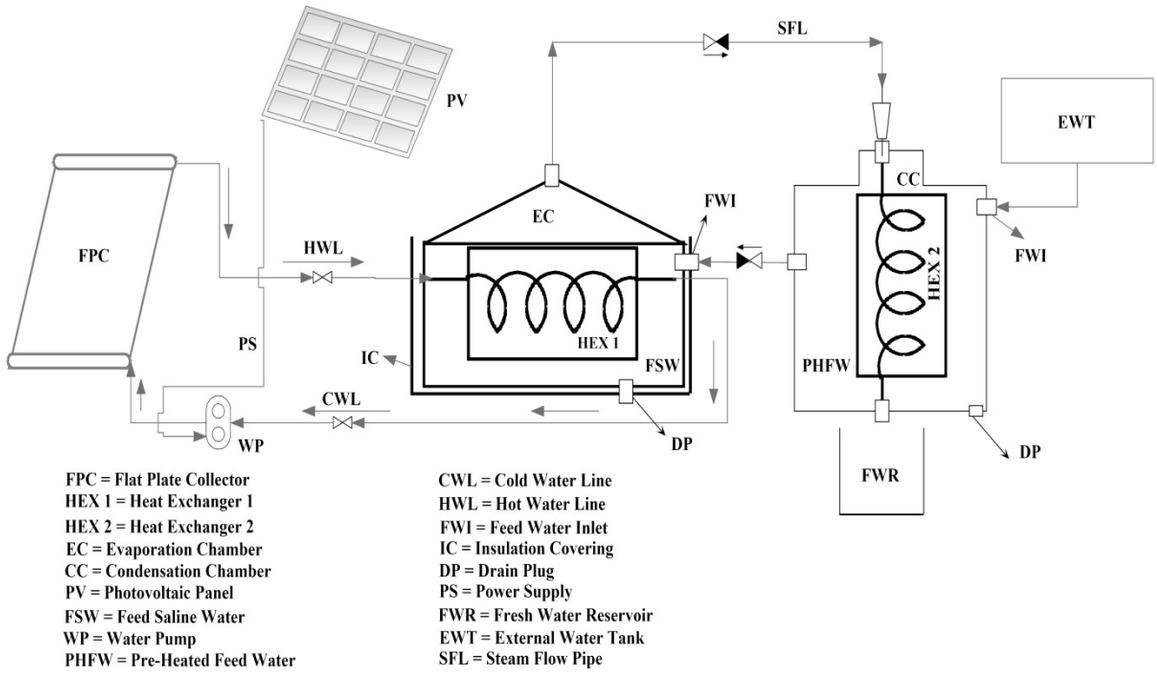

Fig. 1. Schematic diagram of solar water desalination system.

passed through the CC and the heat of vapors is recovered using fresh water supply and the condensed vapors are collected from the bottom. The designed system works under atmospheric pressure using hot water from FPC to produce distillate. Using heat recovery method, the feed water for EC is pre-heated in the CC using latent heat of condensation of water vapors.

To measure the performance of the system, solar radiation, FPC inlet and outlet temperatures, EC and CC temperatures, mass flow rates and heat losses from the system have been measured. The performance evaluation of solar desalination system has been carried out under local climatic conditions at University of Agriculture, Faisalabad, Pakistan. The energy breakdown analysis is performed for each component including the FPC, the EC and CC using different equations. The changes in concentration were assumed to be insignificant. The following relevant equations were used [32]. The total power available (Q_{in}) for the FPC can be calculated using Eq. (1)

$$Q_{in} = I_t \, x \, A_c \tag{1}$$

The total power converted (Q_u) by FPC is the rate of heat extraction from the collector by the means of the heat carried away by the fluid passing through it and can be calculated using Eq. (2).

$$Q_u = \frac{MFR \times c_p \times \Delta T}{t} \tag{2}$$

The collector efficiency (η) is the ratio of the useful energy produced (Q_u) to the total incident solar energy on the collector (Q_{in}) over a specific period of time and can be calculated using Eq. (3).

$$\eta = \frac{Q_u}{Q_{in}} \times 100 \tag{3}$$

The EC efficiency refers to the utilization of heat of the circulating fluid coming from FPC by the feed water for its conversion into vapors and it is estimated by using the inlet/outlet data of FPC for Q_{in} and EC inlet/outlet data for Q_u in the loop [Eq. (3)]. The CC efficiency refers to the amount of heat content recovered from the vapors before leaving the system and it is estimated by comparing the total amount of heat carried by the vapors entering the CC and the total heat taken away by the water leaving the system. The overall efficiency of the system is estimated as the product of all three efficiencies.

2.1. Instrumentation

The thermocouples and thermometers were employed at different position in the system to measure temperatures of inlet and outlet water in EC and CC, inlet and outlet temperatures of FPC, and ambient temperature. The daily solar radiation data has also been recorded using pyranometer. The mass flow rate through the collector is regulated manually using a control valve (regulator) and is measured using a flow meter. The current and voltage of the pumps were monitored using a digital meter. A graduated tank has been used to measure the amount of hourly and cumulative desalinated water having range of 0–10 l with ±0.01 l accuracy. The quality tests of feed water and distilled water have been carried out using pH meter, EC meter, water quality analyzer and other necessary instruments to determine the concentration of drinking water quality parameters including total dissolved solids (TDS), electrical conductivity (EC), pH, boron,

calcium, sodium, sulphates, fluoride, magnesium and chlorine, arsenic, E coli and facial coliform in distillate.

3. Results and discussion

The performance evaluation of solar desalination has also been carried out to test the feasibility of the system for desalination purpose. The data has been collected on daily basis starting from 09:00 am to 04:00 pm during summer season when the solar radiation vary from 450 to 850 W/m^2. To understand the system's behavior during operation, the system is operated by varying different parameters on randomly selected days during summer and the sample data recorded on a clear sunny day is shown in Table 1. The major experimental parameters includes collector tilt angle, mass flow rate, FPC inlet and outlet temperature, EC and CC water temperature and solar irradiance have a direct influences on the system overall productivity and efficiency and all the required data of different parameters were recorded precisely at an interval of 60 min. There are also some other parameters that affect the system productivity such as ambient temperature, salinity of feed water and wind speed etc. But these factors have minor effects on the productivity. The hourly and cumulative productivity was also measured.

3.1. Variation in daily solar radiation and ambient temperature

The variation in hourly ambient temperature and solar irradiance measured on different days in summer season is shown in Fig. 2. It is depicted from the figure that the ambient temperature on May 28, 2015 increases rapidly between 11:00 am to 12:00 pm while a rapid increase in temperature on June 7, 2015 is observed between 10:00 am to 11:00 am. It is also important to mention that the variation in ambient temperatures is due to change in other climatic factors like solar radiation, wind speed, humidity and clouds etc. It is also depicted from the figure that ambient temperature is higher at 12 noon when solar radiation is maximum. The solar radiation increases directly with daytime in peak sunshine hours up to 02:00 pm and then it decreases gently in the evening. The mean daily global radiation for different days of summer season was found to be in the range of 600 W/m^2 to 700 W/m^2. It was inferred that the radiation is high on May 28, 2015 as compared to other two days. This may be due change in solar declination angle or due to the blockage of beam radiation by clouds or humidity which caused lower the total solar radiation.

3.2. Effect of MFR and tilt angle on FPC inlet and outlet temperatures

The variation in the inlet and outlet temperature of FPC measured on different days at two different FPC tilt angles (30° and 40°) and three MFR (0.03 kg/s, 0.04 kg/s, 0.05 kg/s) has been shown in Fig. 3. It is inferred from the figure that the tilt angle has significant effect on outlet temperature of FPC. The outlet water temperature of FPC in case of 30° tilt angle was higher as compared to 40° tilt angle for all MFR. The figure also shows that the rate of increase in FPC inlet temperature for initial 300 min from start of the experiment was higher because large temperature difference exists between inlet and outlet temperatures of FPC and ambient temperature. The rate of increase in the inlet temperature becomes nearly constant after 360 min. This is due to the fact that the fixed amount of water inside the EC is heated and the rate of energy utilization in EC decreases. The FPC outlet temperature is higher at noon when solar irradiance is usually higher. The effect of MFR was also found to be significant. For all three MFR, the trend of FPC inlet and outlet temperatures variation was observed similar but it is depicted from

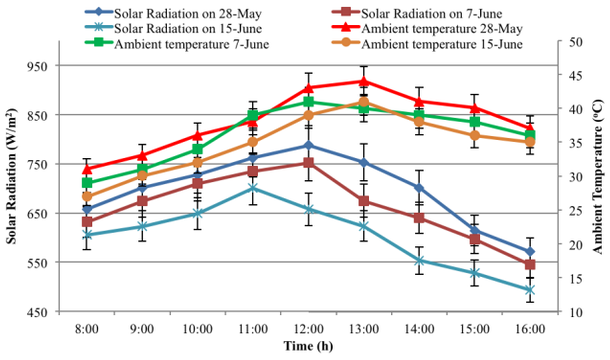

Fig. 2. Variation in solar irradiance and ambient temperature.

Table 1
Data log sheet for solar desalination system using FPC 30°N tilt angle @ 0.04 kg/s

Time	Radiation (W/m^2)	FPC inlet temp (°C)	FPC outlet temp (°C)	EC outlet temp (°C)	Pipe temp (°C)	CC temp (°C)	Ambient temp (°C)	Hourly productivity (L)	Cumulative productivity (L)
8:00	631.45	29	64	29	47	28	31	0.24	0.24
9:00	674.70	33	68	33	49	32	33	0.38	0.62
10:00	709.30	37	72	38	51	35	36	0.49	1.11
11:00	735.25	42	76	43	55	41	38	0.54	1.65
12:00	752.55	46	79	47	58	45	43	0.58	2.23
13:00	674.70	51	82	52	60	48	44	0.59	2.82
14:00	640.10	53	78	56	63	52	41	0.57	3.39
15:00	596.85	55	72	60	63	54	40	0.55	3.94
16:00	544.95	58	64	63	61	56	37	0.53	4.47

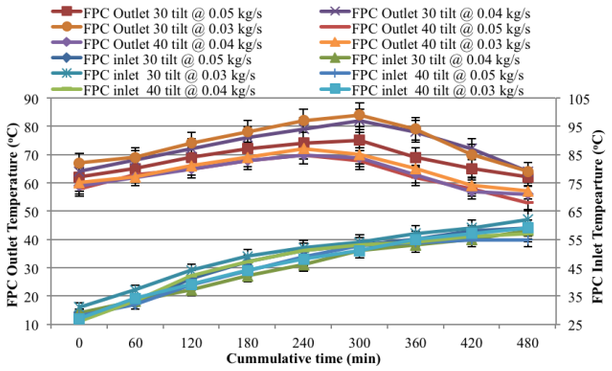

Fig. 3. Effect of MFR and tilt angle on FPC inlet and outlet temperatures.

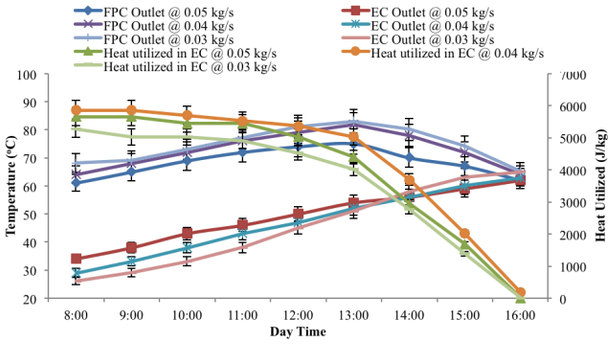

Fig. 4. Effect of MFR on FPC outlet and EC temperature and heat utilized.

the figure that when MFR of 0.03 kg/s was employed for both tilt angles, the maximum value was recorded for outlet temperature. The gain in temperature is due to the fact that traveling time of a single water molecule is increased and it allows transferring most of the heat to the moving fluid. However, the rate of heat extraction for utilization in EC was reduced and the losses were increased. In case, when MFR 0.05 kg/s is set, the rate of heat extraction is increased and the efficiency is also on a higher side but travel time across FPC was reduced thus not allowing water to attain maximum temperature. The MFR 0.04 kg/s was found to be optimum due to the fact that, the outlet temperature was found to be maximum as compared to temperature achieved at MFR 0.03 kg/s while the rate of heat extraction for utilization was nearly as high as in MFR 0.05 kg/s. The maximum thermal efficiency was also achieved at optimum MFR of 0.04 kg/s. The figure also shows that the inlet and outlet temperatures of FPC coincide after 480 min from start of the experiment which resulted thermal losses to the environment due to lower solar irradiance. Since, the system is operated using continues flow pump, therefore the further operation of the system is of no benefit as the FPC outlet temperature falls below than the temperature inside the EC.

3.3. Effect of MFR and FPC tilt angle on heat utilization in EC

The FPC and EC outlet temperatures and heat energy utilized by water in EC at different MFR is shown in Fig. 4. The figure shows that the maximum rate of increase in outlet temperature of FPC was measured from 10:00 am to 12:00 pm and then decreases continuously. The rate of increase in EC increases during the day. It is due to the fact that at start of the experiment the temperature difference (ΔT) between FPC outlet temperature and EC is higher and both coincide around 04:00 pm. It is inferred from the figure that EC temperature at MFR of 0.04 kg/s and 0.05 kg/s exhibits similar results having slightly higher values for MFR 0.05 kg/s. It is due to the fact that at higher MFR, heat content carried by the moving fluid in HEX was not transferred to water in EC and moving fluid leaves the EC at slightly higher temperature. The outlet temperature of EC at MFR 0.03 kg/s exhibits different results which was lower at start of the experiment and increases abruptly at noon time. It is due to the fact that lower MFR allow moving fluid in HEX to transfer all the heat content to water in EC but when the temperature difference (ΔT) decreases, the heat flow from HEX to EC become insignificant resulting in slightly higher values for EC outlet temperature. It is also depicted from the figure that heat utilized at MFR 0.04 kg/s is more as compared to other MFRs due to the fact that lower EC outlet temperature refers higher heat utilized by the water. As the temperature of the water in the EC increases, the rate of utilization of heat energy decreases during the day and reaches to zero at 04:00 pm. Afterwards, the heat energy starts to flow from EC to the FPC. At this stage, the operation of the pump should be switched off to reduce the thermal losses to the ambient environment.

3.4. Effect of MFR on CC temperature and heat recovered

The variation in pipe temperature, CC temperature and heat energy recovered in CC at different MFR is shown in Fig. 5. It is depicted from the figure that the increase in the rate of pipe and CC temperature was observed from 120 to 300 min from start of the experiment. Afterwards, the rate of increase in the temperature becomes constant and then decreases gradually. It is due to the fact that at start of the experiment, the temperature difference (ΔT) between the pipe outlet and CC was higher. It is also depicted from the figure that pipe and CC temperature at MFR 0.04 kg/s was higher as compared to other two MFRs. It is due to the fact that heat utilization in EC at MFR 0.04 kg/s is higher that allows more vapors production which then transferred to the CC through pipe resulting in slightly higher pipe temperature as compared to other MFRs considered in this study. The higher pipe temperature results in higher CC temperature due to the fact more vapors enters the CC and releasing their latent heat as the productivity of the system is highest at MFR 0.04 kg/s. It is also inferred from the figure that heat recovered from the vapors entering CC was calculated to be 1500 J/kg at start of the experiment and decreases to 400 kJ/kg after 480 min. After 360 min, the both water reaches to equilibrium state and the rate of heat exchange decreases.

3.5. Effect of MFR on hourly efficiency of components

The variation in hourly efficiency of the system at MFR 0.04 kg/s is shown in Fig. 6. It is important to mention here

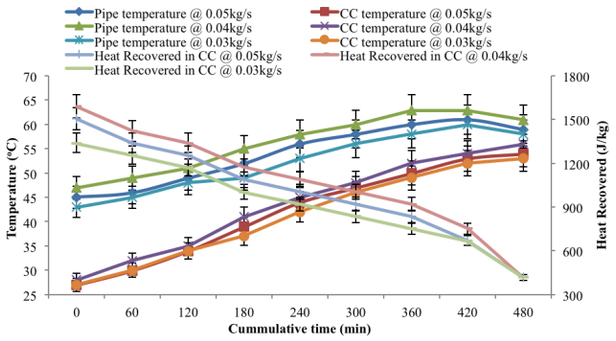

Fig. 5. Effect of MFR on pipe and CC temperatures and heat recovered.

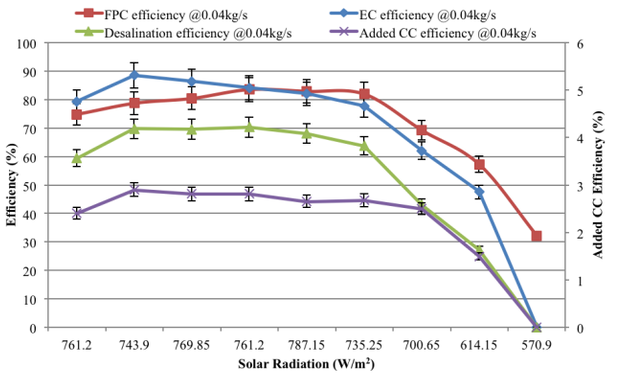

Fig. 6. Variation in hourly efficiency of each system component.

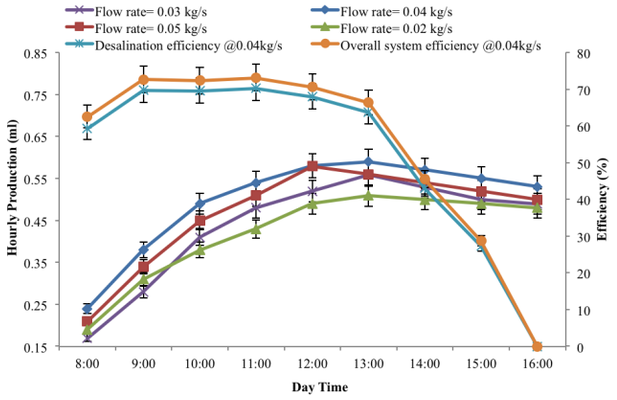

Fig. 7. Variation in hourly efficiency and hourly distillate productivity.

that FPC efficiency was higher than EC efficiency due to the fact that heat carried by the moving fluid from FPC is not fully utilized by the EC and moving fluid leaves the EC at higher temperature. It is concluded from the figure that EC efficiency at start of the experiment was higher than FPC due to the fact that FPC was not directly facing the sun in morning hours due to absence of tracking mechanism thus resulting lower FPC efficiency and also EC temperature is very low in the start and it utilizes most of the heat energy coming from FPC. It is also depicted from the figure that the efficiency of FPC, EC and desalination increases from start of the experiment. Afterwards the efficiency curves show a declining trend. This is due to the fact that ΔT is higher at start of the experiment resulting higher rate of heat extraction, transfer and utilization in FPC and EC. Later on, the ΔT continuously decreases as the system works resulting decreased rate of heat extraction and utilization which results lower efficiency of the system during noon hours. It is worth mentioning here that the system efficiency has been improved by the addition of CC to recover the heat of moving vapors. The incremental efficiency by CC was found to be constant up to noon, decline after noon and eventually end up on zero in the evening due to lower FPC, EC efficiency and lower vapor production.

3.6. Effect of MFR on hourly distillate productivity and efficiency

The hourly distillate productivity rate at different MFR for different summer season days is shown in Fig. 7. The figure shows that MFR has a significant effect on distillate productivity of the system. The maximum water productivity was measured at MFR of 0.04 kg/s as compared with 0.02, 0.03 and 0.05 kg/s. The maximum water productivity was found at 01:00 pm at MFR of 0.04 kg/s due to the fact that the rate of EC heat utilization and CC heat recovery was higher for the given MFR. The higher distillate productivity was also due to the fact that solar radiation was maximum at noon time. The average distillate production was found to be 0.42, 0.43, 0.49 and 0.46 l/h from lower to higher MFRs respectively. This is due to the fact that at low MFR, the thermal losses from FPC increases since all the heat energy is not carried away by the heat transfer medium. The distillate productivity was lower at start of the experiment because most of sensible heat was used to increase the initial water temperature to initiate evaporation process. The figure also shows that the distillate productivity was higher in the afternoon period as compared with the time before 12:00 pm. The figure also shows the efficiency curve of system at MFR 0.04 kg/s (maximum productivity). It is concluded from the figure that hourly efficiency of the system was found to be maximum in the range of 60 to 65% for the period between 09:00 am to 01:00 pm and decreases afterwards. It is due to the fact that at start of the experiment, the collector was directly facing the sun, most of the radiation is captured by FPC and heat energy from FPC outlet is utilized by EC as the ΔT between them was higher. The system efficiency reaches to zero at 04:00 pm due to the fact that equilibrium was achieved and heat energy starts flowing from EC to FPC. It is worth mentioning here that, the heat recovery in CC resulted increase in the system efficiency in the range of 3 to 6%.

3.7. Effect of MFR on gain output ratio, average efficiency and distillate yield

The distillate yield and daily mean efficiency at different MFR during summer season is shown in Fig. 8. The figure shows that the MFR has a significant effect on the productivity and efficiency of the system. The maximum distillate

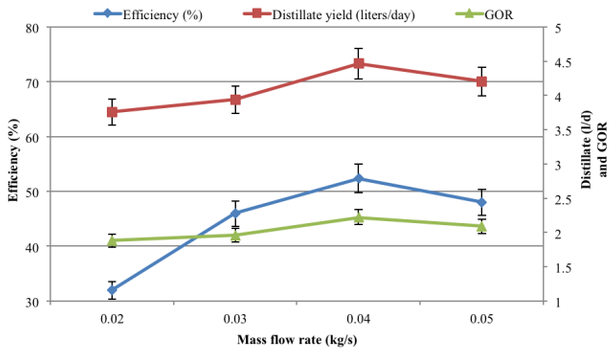

Fig. 8. Effect of MFR on daily productivity, mean efficiency and GOR.

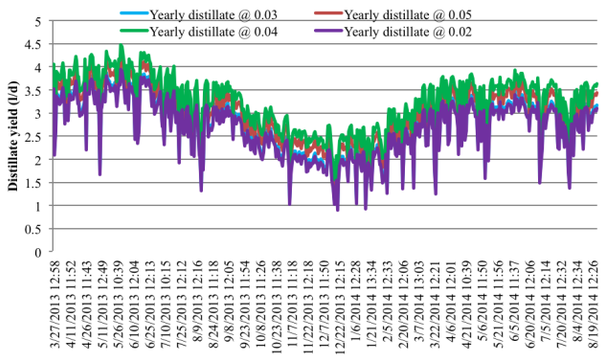

Fig. 9. Variation of daily distillate production at different MFR.

at MFR of 0.05, 0.04, 0.03 and 0.02 kg/s was found to be 4.21, 4.47, 3.94 and 3.76 l/m^2 with mean daily efficiency as 32, 46, 52 and 48% respectively. The maximum mean daily system efficiency reaches to 52% at MFR of 0.04 kg/s which was found to be higher for existing similar studies. It is due to the fact that lower MFR results higher thermal losses from the system thus reducing distillate production and efficiency of the system. It is important to mention that heat recovery of vapors in CC results 6% increase in efficiency of the system. The performance or energy efficiency of system depends on the operation conditions and is measured as the gain output ratio (GOR). The GOR of the system at different MFR is also shown in Fig. 8. Based on energy input and energy output relationship as reported by [33], the GOR is calculated using Eq. (4).

$$GOR = \frac{M_e \, x \, h_{fg}}{Q_{in}} \tag{4}$$

Higher values of GOR refer high energy efficiency and more distillate yield. The GOR of this system reached in the range of 1.7 to 2.2, indicating that the CC successfully recovers the latent heat of vapors condensation. It is concluded from the figure that the influence of MFR on GOR is very low because variation in MFR has negligible effect on heat recovery in CC.

3.8. Annual distillate yield at different MFR

The annual distillate production at different MFR has also been investigated as shown in Fig. 9. The figure shows that the system is capable to produce continuous distillate around the year but the distillate production is lower in winter season. It is due to the fact that during winter season solar radiation and ambient temperature are lower to start the evaporation process while more than 300 sunny days are capable to produce continuous and higher amount of distillate. It is also depicted from the figure that the system distillate productivity was found to be highest at MFR of 0.04 kg/s and the annual distillate yield approximated 1500 L within stated operating parameters. Moreover, the tilt angle of FPC also affects distillate yield and the maximum distillate was found at latitude of the location.

3.9. Water quality analysis

After the desalination of brackish water, the water quality tests have also been performed to test the suitability of the distillate for drinking purposes. The results have also been compared with water quality standards defined by WHO in Table 2. The table shows that the total dissolved solids (TDS) remarkably decreased from 2640 to 188 ppm after desalination process. The presence of small amount of TDS after desalination may be due to existence of volatile compounds which evaporate at lower temperatures due to its lower boiling points. Similarly, the electrical conductivity (EC), pH, Boron, Arsenic, calcium, sodium, sulphates, fluoride, magnesium, chlorine, *E. coli* and facial coliform concentration has also been decreased and was found to be in the range of WHO standards set for drinking water quality.

3.10. Cost analysis

For economic feasibility of the system, the cost analysis of the solar desalination system has also been performed using different equations. The cost breakdown of the system is shown in Table 3. Considering life of the system components (FPC, EC, CC, PV panel) as 20 y (reusable materials) and annual interest rate (*i*) as 12%, the capital recovery factor (CRF) and sinking fund factor (SFF) can be calculated using Eqs. (5) and (6) [34–36].

$$CRF = \frac{i(1+i)^n}{\left[(1+i)^n - 1\right]} \tag{5}$$

$$SFF = \frac{i^n}{\left[(1+i)^n - 1\right]} \tag{6}$$

The first annual cost (FAC) is calculated using initial investment (P) as shown in Eq. (7). A pump has a shorter life since it has mechanical components with moving parts and is not considered as reusable material [37]. The Annual salvage value (ASV) is calculated using the salvage value (S) as zero for the non-reusable material and 50% for reusable materials using Eq. (8).

$$FAC = P \; x \; CRF \tag{7}$$

Table 2
Water quality analysis and comparison with International Standards

Parameters	Feed water	Distillate	WHO drinking water guidelines
pH	7.1	6.7	6.5–8.5
Total dissolved solids (mg/l)	2640	188	500
Electrical conductivity (μS/cm)	547	96	1000
Boron (mg/l)	0.1	0.02	0.3
Arsenic (mg/l)	0.03	*	0.01
Calcium (mg/l)	52.2	28.6	100
Sodium (mg/l)	31.5	20.7	100
Sulphates (mg/l)	72.4	36.8	250
Fluoride (mg/l)	0.8	0.5	1.5
Magnesium (mg/l)	27.4	11.5	50
Chlorine (mg/l)	5.8	2.1	5
E. coli and facial coliform	2.45 and 2.09	*	*

*Not detectable in 100 ml sample.

Table 3
Cost breakdown of solar desalination system

System Component	Cost (US $)
FPC	80
EC	25
CC	25
PV panel	60
Pump	25
Insulation	05
Total	220

$$ASV = SFF\ x\ S \tag{8}$$

The annual energy consumption (E_v) and annual running cost (ARC) can be calculated as a result of operational time (t) and electricity price (Z) as shown in Eq. (9) and Eq. (10). The system comprises a DC pump powered by PV panel resulting no running cost of the system.

$$E_v = 365\,x\,W_{pump}\,x\,t \tag{9}$$

$$ARC = E_v\,x\,Z \tag{10}$$

The annual maintenance cost (AMC) is considered 20% of FAC and is calculated using Eq. (11) [2]. The annual cost (AC) is calculated using Eq. (12).

$$AMC = 0.20\,x\,FAC \tag{11}$$

Table 4
Cost analysis of solar desalination system

n (years)	20
i (%)	12
P (US $)	220
S (US $)	95
CRF	0.134
SFF	0.014
FAC (US $)	29.48
ASV (US $)	1.33
Z (US $)	0
ARC (US $)	0
AMC (US $)	5.9
AC (US $)	34.05
AY (liter)	1500
Cost/ liter (US $)	0.021
Cost/ liter (PKR)	1.98
Payback (years)	2.26

$$AC = FAC + AMC + ARC - ASV \tag{12}$$

The cost of distillate is estimated assuming 250 operating days. Cost of distillate per liter is finally calculated using Eq. (13). The payback time of the system depends on total life time investment (P and AMC) and it is estimated using Eq. (14).

$$\text{Cost per liter} = \frac{AC}{AY} \tag{13}$$

$$\text{Payback} = \frac{\text{Investment}}{\text{Total city pure water price}} \tag{14}$$

Since this small scale distillation system has been designed to serve domestic purpose in the remote areas of the country having water scarcity. Thus, the proposed desalination system uses low cost equipment and has higher efficiency and distillate productivity due induction of heat recovery CC unit and the cost of the system is $220 which is affordable to local community. Considering life of system, the cost per liter of water from the system is $0.021 which is much lower than the cost of fresh water available to remote areas. The summary of cost analysis is shown in Table 4.

4. Conclusions

The environmental consequences associated with the use of fossil fuels have now realized the world to explore alternate sources of energy which might be long lasting and have no emissions. In this connection, carbon credit policy has already been adopted by developed countries. It is the time that the developing countries should also play their role by the exploitation of these natural resources in order to reduce the carbon emission and making this world a green

globe. Pakistan is facing severe problem of energy shortage and fresh water supply. In the meanwhile, the availability of solar insolation in the range of 5–5.5 kWh/m^2 in most parts of the Pakistan offers an excellent opportunity to effectively use it to overcome energy crises and for desalination purpose. In this way, Pakistan can also play its role to reduce carbon emission. Desalination using membrane technology requires huge amount of energy and thermal desalination technologies usually result in low distillate productivity with lower efficiency. So, this study has been carried out for the development and evaluation of solar desalination system using evaporation condensation and heat recovery method. The result shows that the system efficiency and water productivity of the system depends on solar radiation, FPC tilt angle, MFR and inlet hot water temperature. The daily water productivity was found to be 4.5 l/m^2 during testing period and the water quality tests shows that the quality parameters are in line with International Water Quality Standards and was found to be EC 96 µS/cm, pH 6.7, TDS 188 ppm while boron, calcium, sodium, sulphate, fluoride, magnesium and chlorine as 0.02, 28.6, 20.7, 36.8, 0.5, 11.5 and 2.1 mg/l respectively. The concentration of arsenic, *E. coli* and facial coliform remained undetectable in the distillate. The system achieves an overall efficiency 52% with the induction of CC. The cost per liter of water from the system is found to be $0.021 approx. which is lower than the city fresh water cost. It is concluded from this study that the solar desalination system can effectively be used for water treatment in most parts of the country.

Acknowledgements

The authors wish to thank German Academic Exchange Service (DAAD), International Work for Development and Decent Work (ICDD) Germany and Higher Education Commission (HEC), Islamabad, Pakistan for the research and financial support. This work has been conducted in the Workshop of Faculty of Agricultural Engineering and Technology, University of Agriculture, Faisalabad-Pakistan.

Symbols

AD	—	Adsorption desalination
A	—	Area of collector in m^2
AC	—	Annual cost
AMC	—	Annual maintenance cost
ARC	—	Annual running cost
ASV	—	Annual salvage value
AY	—	Annual yield
CC	—	Condensation chamber
CRF	—	Capital recovery factor
EC	—	Evaporation chamber
EPA	—	Environmental protection agency
E_v	—	Annual energy consumption
FAC	—	First annual cost
FPC	—	Flat plate collector
GOR	—	Gain output ratio
HEX	—	Heat exchanger
HDH	—	Humidification–dehumidification desalination
I_t	—	Total solar irradiance in W/m^2
i	—	Annual interest rate
h_{fg}	—	Latent heat of vaporization kJ/kg
M_e	—	Fresh water production in liters
MFR	—	Mass flow rate in kg/sec
MED	—	Multi effect distillation
MSF	—	Multi stage flash
n	—	System life in years
P	—	Initial investment
PV	—	Photovoltaic
Q_{in}	—	Total power available in W
Q_u	—	Total useful energy in W
RO	—	Reverse osmosis
C_p	—	Specific heat of water in kJ/kg°C
S	—	Salvage value
SFF	—	Sinking fund factor
t	—	Time interval in sec
TC	—	Thermal conductivity
TDS	—	Total dissolved solids
W_{pump}	—	Pump power in W
Z	—	Electricity price
ΔT	—	Temperature difference in °C
η	—	Efficiency (%)

References

[1] Desalination Markets 2005–2015, A global assessment and forecast, Global Water Intelligence 2005.
[2] H.T. El-Dessouky, H.M. Ettouney, A text Book on Fundamentals of salt water desalination, Elsevier, 2002.
[3] S.A. Kalogirou, Seawater desalination using renewable energy sources, Progr. Energy Combust. Sci., 31 (2005) 242–281.
[4] M.S. Abu Jabal, I. Kamiya, Y. Narasaki, Proving test for a solar powered desalination system in Gaza, Palestine, Desalination, 137 (2001) 14–16.
[5] B. Bouchekima, Solar desalination plant in small size in remote arid areas of South Algeria for production of drinking water, Desalination, 154 (2003) 1–7.
[6] R. Dashtpour, S.N. Al-Zubaidy, Energy efficient reverse osmosis desalination process, Int. J. Environ. Sci. Dev., 3(4) (2012) 339–345.
[7] M. Khayet, Solar desalination by membrane distillation dispersion in energy consumption analysis and water production costs, Desalination, 308 (2012) 89–101.
[8] R.L. Garcia, Seawater desalination driven by renewable energies: a review, Desalination, 143 (2002) 103–113.
[9] M.S. Khalil, N.A. Khan, I.A. Mirza, Renewable energy in Pakistan: Status and trends, University of Engineering and Technology, Taxila, Pakistan, 2003.
[10] H. Sharon, K.S. Reddy, A review of solar energy driven desalination technologies, Renew. Sustain. Energy Rev., 41 (2012) 1080–1118.
[11] M. Shatat, M. Worall, S. Riffat, Opportunities for solar water desalination worldwide review, Sustain. Cit. Soc., 9 (2013) 67–80.
[12] C. Li, Y. Goswami, E. Stefanakos, Solar assisted sea water desalination review, Renew. Sustain. Energy Rev., 19 (2013) 136–163.
[13] C. Fritzmann, J. Loewenberg, T. Wintgens, T. Melin, State-of-the-art of reverse osmosis desalination, Desalination, 216 (2007) 1–76.
[14] A. Frankel, Flash evaporators for distillation of sea water, Proc. Inst. of Mech. Eng., 174 (1960) 312–324.
[15] J. Joseph, R. Saravanan, S. Renganarayanan, Studies on a single-stage solar desalination system for domestic applications, Desalination, 173 (2005) 77–82.
[16] H.M. Qiblawey, F. Banat, Solar thermal desalination technologies, Desalination, 220 (2008) 633–644.
[17] R.B. Saffarini, E.K. Arafat, H.A. Lienhard, Technical evaluation of stand-alone solar powered membrane distillation systems, Desalination, 286 (2012) 332–341.

[18] L. Zhang, H. Zheng, Y. Wu, Experimental study on a horizontal tube falling film evaporation and closed circulation solar desalination system, Renew. Energy, 28 (2003) 1187–1199.
[19] A.F. Mashaly, A.A. Alazba, A.M. Al-Awaadh, Assessing the performance of solar desalination system to approach near-ZLD under hyper arid environment, Desal. Water Treat., 57 (2016) 12019–12036.
[20] A.E. Kabeel, E.M.S. El-Said, Applicability of flashing desalination technique for small scale needs using a novel integrated system coupled with nano-fluid-based solar collector, Desalination, 333 (2014) 10–22.
[21] Y. Kim, K. Thu, M.E. Masry, K.C. Nig, Water quality assessment of solar-assisted adsorption desalination cycle, Desalination, 344 (2014) 144–151.
[22] Z.H. Liu, R.L. Hu, X.J. Chen, A novel integrated solar desalination system with multi-stage evaporation/heat recovery processes, Renew. Energy, 64 (2014) 26–33.
[23] S.A. El-Agouz, G.B. Abd El-Aziz, A.M. Awad, Solar desalination system using spray evaporation, Energy, 76 (2014) 276–283.
[24] N.K. Nawayseh, M.M. Farid, S. Al-Hallaj, A.R. Al-Timimi, Solar desalination based on humidification process. Evaluating the heat and mass transfer coefficients, Energy Convers. Manage., 40 (1999) 1423–1439.
[25] A.E. Kabeel, E.M.S. Emad, A hybrid solar desalination system of air humidification–dehumidification and water flashing evaporation, Desalination, 320 (2013) 56–72.
[26] A.S. Nafey, H.E.S. Fath, S.O. El-Helaby, A. Soliman, Solar desalination using humidification–dehumidification processes Part II. An experimental investigation, Energy Convers. Manage., 45 (2004) 1263–1277.
[27] J.J. Hermosillo, C.A. Arancibia-Bulnes, C.A. Estrada, Water desalination by air humidification: Mathematical model and experimental study, Sol. Energy, 86 (2012) 1070–1076.
[28] S. Farsad, A. Behzadmehr, Analysis of a solar desalination unit with humidification–dehumidification cycle using DoE method, Desalination, 278 (2011) 70–76.
[29] K. Zhani, H. Ben-Bacha, Experimental investigation of a new solar desalination prototype using the humidification dehumidification principle, Renew. Energy, 35 (2010) 2610–2617.
[30] S. Parekh, M.M. Farid, J.R. Selman, S. Al-Hallaj, Solar desalination with a humidification dehumidification technique: a comprehensive technical review, Desalination, 160 (2004) 167–186.
[31] A. Shariah, M.A. Al-Akhras, I.A. Al-Omari, Optimizing the tilt angle of solar collectors, Renew. Energy, 26 (2002) 587–598.
[32] L.G. Rodriguez, C.G. Camacho, Energy analysis of SOL-14 plant, Desalination, 137 (2001) 251–258.
[33] Z. Chang, H. Zheng, Y. Yang, Y. Su, Z. Duan, Experimental investigation of a novel multi-effect solar desalination system based on humidification-dehumidification process, Renew. Energy, 69 (2014) 253–259.
[34] A.E. Kabeel, A.M. Hamed, S.A. El-Agouz, Cost analysis of different solar still configurations, Energy, 35 (2010) 2901–2908.
[35] H.E.S. Fath, M. El-Samanoudy, K. Fahmy, A. Hassabou, Thermal-economic analysis and comparison between pyramid-shaped and single-slope solar still configurations, Desalination, 159 (2003) 69–79.
[36] Govind, G.N. Tiwari, Economic analysis of some solar energy systems, Energy Convers. Manage., 24 (1984) 131–135.
[37] A.S.E. Nabil, F.R. Siddiqui, G.I. Sultan, Development of a desalination system driven by solar energy and low grade waste heat, Energy Convers. Manage., 103 (2015) 28–35.